Screening of hub genes and evaluation of the growth regulatory role of CD44 in metastatic prostate cancer

JUNHAO LIN, ZHI CHEN, ZUAN LI, DEYONG NONG, XIMING LI, GUIHAI HUANG, NAN HAO, JIANBO LIANG and WEI LI

Department of Urology, The People's Hospital of Guangxi Zhuang Autonomous Region, Nanning, Guangxi Zhuang Autonomous Region 530021, P.R. China

Received October 16, 2020; Accepted May 12, 2021

DOI: 10.3892/or.2021.8147

Abstract. Prostate cancer (PCa) is the most common cancer type in men worldwide. Currently, the management of metastatic PCa (mPCa) remains a challenge to urologists. The analysis of hub genes and pathways may facilitate the understanding of the molecular mechanism of PCa. In the present study, to identify the hub genes in the mPCa, the three datasets GSE3325, GSE6919 and GSE38241 were downloaded from the platform of the Gene Expression Omnibus and function enrichment analysis of differentially expressed genes (DEGs) was performed. A total of 168 DEGs were obtained and the DEGs were significantly enriched in 'cell junction' and 'cell adhesion', among others. The Kyoto Encyclopedia of Genes and Genomes pathway enrichment analysis demonstrated that DEGs were enriched in three pathways including 'focal adhesion', 'renal cell carcinoma' and 'Hippo signaling pathway'. The results of the protein-protein interaction network revealed that the hub genes in mPCa were separately PTEN, Rac GTPase-activating protein 1, protein regulator of cytokinesis 1, PDZ binding kinase, centromere-associated protein E, NUF2 component of NDC80 kinetochore complex, TPX2 microtubule nucleation factor, SOX2, CD44 and ubiquitin-like with PHD and ring finger domains 1. As a hub gene, CD44 was differentially expressed in PCa, as determined by Oncomine analysis. Further experiments *in vivo* demonstrated that SB-3CT, a selective matrix metalloproteinase inhibitor that has been reported to block CD44 cleavage and inhibit the downstream signaling pathway, suppressed the tumorigenicity of PCa cells by decreasing the expression levels of pyruvate dehydrogenase kinase 1 and 6-phosphofructo-2-kinase/fructose-2,6-biphosphatase 4. Moreover, the combination therapy with SB-3CT and docetaxel was more effective in inhibiting PCa compared with monotherapy. In conclusion, the identification of DEGs and the *in vivo* experimental results helped to elucidate the molecular mechanisms of PCa and provided a potential strategy for the treatment of PCa.

Correspondence to: Dr Wei Li, Department of Urology, The People's Hospital of Guangxi Zhuang Autonomous Region, 6 Taoyuan Road, Nanning, Guangxi Zhuang Autonomous Region 530021, P.R. China
E-mail: liwei95_2000@163.com

Key words: bioinformatics analysis, hub gene, CD44, prostate cancer

Introduction

Prostate cancer (PCa) is the second most common cancer type worldwide and was ranked fifth with regards to cancer-related mortality rates in men in 2018 globally (1). Localized PCa can be treated using radical prostatectomy or radiation therapy (2). However, the disease control of metastatic PCa (mPCa) remains unsatisfactory (3). Although hormonal therapy has been widely used for mPCa, recurrence nearly always occurs after the initial period of treatment response and the cancer inevitably progresses to metastasis castrate-resistant PCa, which is extremely difficult to treat (4,5). Therefore, it is crucial to identify the exact molecular mechanism of the progression of mPCa, which may provide novel diagnostic and therapeutic targets.

Over the last decades, the technology of gene microarray and bioinformatic analysis has been applied for the examination of genetic alterations, which has enabled the identification of differentially expressed genes (DEGs) between mPCa and normal prostate tissues (6). In the present study, different microarray datasets were downloaded from the Gene Expression Omnibus (GEO) and multivariate statistical techniques were used for analysis. Analysis of the protein-protein interaction (PPI) network, enrichment analysis of Gene Ontology (GO) and Kyoto Encyclopedia of Genes and Genomes (KEGG) pathway were performed to predict the hub genes and the molecular mechanism of mPCa among the DEGs, which could guide future experiments *in vitro* and *in vivo*.

CD44 is a cell-surface receptor that is expressed in the majority of normal and cancer tissues (7). CD44 is a cell-surface marker that is associated with the stemness, initiation and invasiveness of tumor cells (8). It has been reported that cell adhesion is primarily mediated by the CD44 signaling pathway, which is initiated by cleavages of CD44 ectodomain. Cleavages of CD44 ectodomain induced CD44 intracellular domain cleavage, and the subsequently generated intracellular domain fragment, can regulate signaling transcription (9). It has been revealed that MMPs are involved in the cleavage of CD44 ectodomain (10). Previous findings have observed that PC-3 cells expressed CD44, while LNCaP cells did not (11). It was also reported that CD44 could regulate cell proliferation, invasion and migration

via pyruvate dehydrogenase kinase 1 (PDK1) and 6-phosphofructo-2-kinase/fructose-2,6-biphosphatase 4 (PFKB4) in PCa cells (12). Additionally, MMP inhibitor (SB-3CT) could decrease glycolytic activity via the inhibition of CD44 in PCa cells, and combination therapy with SB-3CT and docetaxel was more effective in inhibiting PCa compared with monotherapy (12).

Based on the results of previous studies *in vitro*, the present study performed additional experiments *in vivo* to further determine the role of CD44 in the progression of PCa and the role of SB-3CT in PCa.

Materials and methods

Information of microarray data. GEO (http://www.ncbi.nlm.nih.gov/geo) is a public repository of high-throughput functional genomics data (13,14). In total, three datasets (GSE3325, GSE6919 and GSE38241) were downloaded from GEO to compare gene expression between metastasis prostate cancer tissues and normal prostate tissues. The organism of the selected datasets was homo sapiens, and the experiment type was expression profiling array. The probes of each dataset were annotated by the gene symbol, according to the information of the platform. The dataset of GSE3325 contained six mPCa tissue samples and six normal prostate tissue samples (15), while GSE6919 contained 25 mPCa tissue samples and 17 normal prostate tissue samples (16,17), and GSE38241 contained 18 mPCa tissue samples and 21 normal prostate tissue samples (18).

Identification of differentially expressed genes. The DEGs between mPCa and normal prostate samples were screened using statistical software R (https://www.r-project.org; version 3.6.0). Data standardization and quality detection were performed prior to analysis. DEGs were identified using the Empirical Bayes method according to the 'limma' package of Bioconductor (https://bioconductor.org) (19). In addition, |log2FC|>1 was set as the cut-off value and adjusted P<0.05 was considered significant. A volcano plot of the DEGs was conducted based on the 'ggplot2' package of R (https://CRAN.R-project.org/package=ggplot2; version 3.2.1). A heatmap of the DEGs was constructed using the 'pheatmap' package of R (https://CRAN.R-project.org/package=pheatmap; version 1.0.12).

Enrichment analysis of GO term and KEGG pathway. GO term enrichment analysis of DEGs including biological process (BP), cellular component (CC) and molecular function (MF) was conducted using the 'clusterProfiler' package of Bioconductor (20). The KEGG pathway enrichment analysis of DEGs was performed using the DAVID database (https://david.ncifcrf.gov; version 6.8), which provides functional annotation tools online for understanding biological processes. P<0.05 was considered to indicate a statistically significant difference (21,22).

Analysis of PPI network and hub gene identification. PPI network analysis was performed to identify hub genes and to evaluate the interactions among DEGs using the online database of Search Tool for the Retrieval of Interacting Genes (STRING; https://string-db.org; version 11.0) and Cytoscape software (www.cytoscape.org; version 3.7.1) (23,24). Firstly, the network of DEGs was mapped using STRING database with an interaction score >0.4. Then, the network was visualized using Cytoscape software. The top 10 hub genes among the DEGs were identified using the cytoHubba plugin of Cytoscape (25).

PCa cell line and cell culture. LNCap and PC-3 cells (obtained from the Cell Bank of Type Culture Collection of Chinese Academy of Sciences) were cultured in RPMI-1640 medium (Thermo Fisher Scientific, Inc.) supplemented with 10% FBS (Thermo Fisher Scientific, Inc.). The cells were cultured in an incubator at 37˚C and 5% CO_2. Negative control groups were designed and performed in the experiments, and experiments were repeated at least three times.

Cell transfection. The sequences of short hairpin (sh)RNA targeting *PDK1* or *PFKFB4* and the negative control were inserted into the lentiviral vector. A non-targeting sequence (forward sequence 5'-CCGGCAACAAGATGAAGAGCACCAACTCGAGTTGGTGCTCTTCATCTTGTTGTTTTT-3') was used as the negative control. Lentiviruses with the packaging plasmid (PG-P1-VSVG, PG-P2-REV, PG-P3-RRE and pGLV3/H1/GFP) and shRNA plasmid were produced via the transfection of 293T cells. Supernatants with lentiviral were collected after transfection and filtered using a 0.45-μm strainer. The lentiviral-expressing CD44 was harvested by inserting the sequences of CD44 into a pLVX-EF1α vector. An empty vector was used as the negative control. The lentiviral vector was used to infect PC-3 cells for 24 h at 37˚C. Using the same method, LNCaP cells were transfected with CD44 overexpression lentiviral vector. PC-3 and LNCaP cells infected by lentiviral vector were cultured for 72 h before subsequent experiments. Plasmid was purchased from BioVector NTCC Inc.

Western blot analysis. Cell extraction was performed using lysis buffer (Thermo Fisher Scientific, Inc.) and protein was separated via 10% SDS-PAGE. The concentration of protein was quantified by the bicinchoninic acid method. The protein extracted from the NC, SB-3CT, SB-3CT + Docetaxel (5 mg/kg), and SB-3CT + Docetaxel (10 mg/kg) groups were loaded in different western blot lanes, respectively. Then, the separated protein was transferred onto a polyvinylidene fluoride membrane. After blocking with 5% skimmed milk, the membrane was incubated with primary antibodies specific for PDK1 (cat. no. ab110025; 1:500 dilution, Abcam), PFKFB4 (cat. no. ab137785; 1:500 dilution, Abcam) or GAPDH (cat. no. ab181602; 1:1,000 dilution, Abcam), followed by incubation with secondary antibody IgG (cat. no. R4880; 1:1,000 dilution, Sigma-Aldrich; Merck KGaA). The protein was visualized using enhanced chemiluminescence and analysed using software by Labworks Analysis Software.

Immunohistochemical staining. Immunohistochemical staining was performed on paraffin-embedded tumor tissue sections using anti-PDK1 (cat. no. ab110025; 1:1,000 dilution, Abcam) or anti-PFKFB4 (cat. no. ab137785; 1:1,000 dilution, Abcam) antibodies according to the manufacturer's protocol. The tissue sample was fixed with 4% paraformaldehyde at 4˚C for 12 h. After staining, the sections (5 μm) were observed at x100 and x400 magnification using a light microscope. Positive cells were distinguished by strong staining of the membrane.

Tumor xenograft model in vivo. Animal experiments were permitted by the Ethics Committee of the People's Hospital of

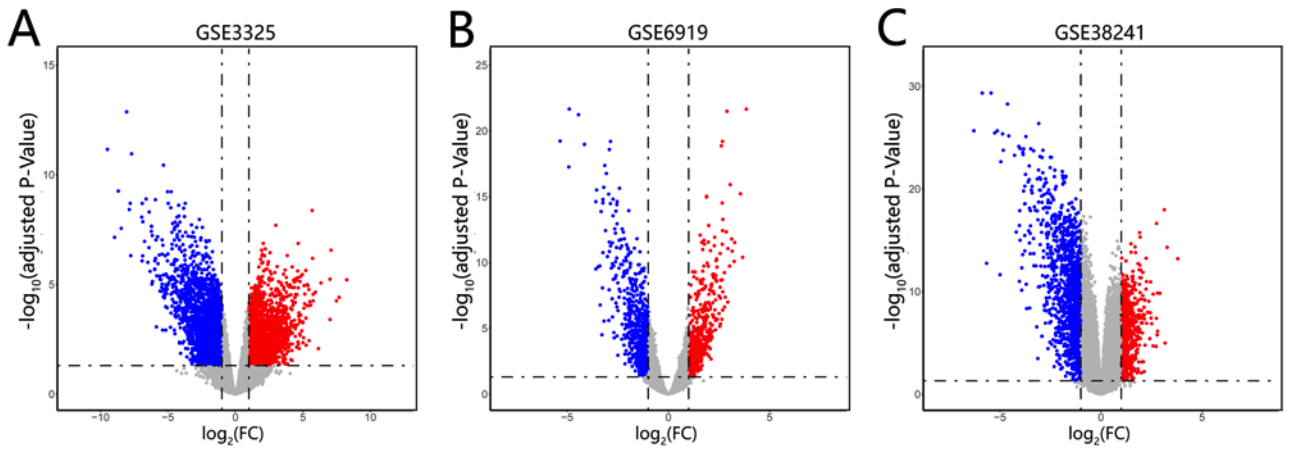

Figure 1. Volcano plots of DEGs. Volcano plots of DEGs in metastasis prostate cancer and normal prostate samples in the datasets of (A) GSE3325, (B) GSE6919 and (C) GSE38241. DEGs were selected using $|\log_2 FC|>1$ and an adjusted $P<0.05$. Colors refer to the different genes: Grey represents genes without significantly different expression. Red represents genes that are upregulated in metastasis prostate cancer tissues compared with normal prostate tissues and blue indicates genes that are downregulated. DEG, differentially expressed genes.

Guangxi Zhuang Autonomous Region (approval no. 2014-010). A total of 40 BALB/c nude mice (age, 4-6 weeks; male; weight, 20-25 g) were obtained from Guangdong Medical Laboratory Animal Center and maintained in a specific pathogen-free environment which consisted of individually ventilated cages and isolator modules. The mice were injected with treated PCa cells in the armpit. PC-3 cells, PC-3 cells infected with shRNA-PDK1 or shRNA-PFKFB4, and LNCaP cells infected with vector-expressing CD44 or negative control were subcutaneously injected into BALB/c nude mice. The BALB/c nude mice injected with PC-3 cells were considered as the negative control. The tumor volume was observed and measured up to 33 days. Tumor weight was measured after mice were euthanized.

For the evaluation of CD44 in the treatment of PCa *in vivo*, PC-3 cells were subcutaneously injected into BALB/c nude mice and SB-3CT or SB-3CT combined with docetaxel (5 or 10 mg/kg) was injected into the mice via the tail vein. The tumor volume and weight were measured, and the tumor tissues were dissected for western blotting and immunohistochemical staining. BALB/c nude mice injected with PC-3 cells were considered the negative control.

During the experiment, 40 BALB/c nude mice were used. Mice were kept on a 12 h light-dark cycle at 50-60% humidity and 23-25˚C and fed chow and water *ad libitum*. The health and behavior of the mice were monitored twice daily, which included weight, water and food intake, and animal posture. Sign of weight loss, rapid breathing, bloating, reduced food intake, and visible tumor under the skin was regarded as illness, which led to the euthanasia of mice. All 40 mice were euthanized as tumors were observed under the skin, using pentobarbital sodium (100 mg/kg) in the study. The pentobarbital sodium was injected via the tail vein. The maximum tumor size in the mice allowed to grow was 2,000 mm^3 (not exceed 20 mm in any direction) before euthanasia. In the research, ulceration of tumors was not observed in any of the mice, and metastatic tumors to the lung were evident in 8 of the 40 mice.

Statistical analysis. The statistical analysis was performed using SPSS software (version 19.0; IBM Corp.) and the graphs were created using GraphPad Prism software (version 6.0; GraphPad Software, Inc.). Data were analysed using the Student's t-test (independent t-test) or a one-way ANOVA with Tukey's post hoc test. $P<0.05$ was considered to indicate a statistically significant difference.

Results

Identification of DEGs in mPCa. The datasets of GSE3325, GSE6919 and GSE38241 were downloaded from the GEO platform. A total of 4,790, 1,144 and 1,920 DEGs were screened from GSE3325, GSE6919 and GSE38241, respectively (Fig. 1A-C). In addition, 168 common DEGs were identified among the three datasets (Fig. 2A) and the expression levels of the common DEGs in the three datasets are presented (Fig. 2B-D).

Enrichment analysis of GO term. The results of GO enrichment analysis varied with regards to the GO term and the different expression of common DEGs (Fig. 3A). The result of GO enrichment analysis in BP showed that the common DEGs were significantly enriched in 'cell junction', 'cell adhesion', 'epithelial to mesenchymal transition' and 'epithelial cell proliferation', among others (Fig. 3B). With regards to CC, the common DEGs were significantly enriched in 'adherens junction', 'cell junction', 'focal adhesion' and 'myofibril', among others (Fig. 3C). For MF, the common DEGs were significantly enriched in 'actin binding', 'collagen binding', 'proximal promoter sequence-specific DNA binding', 'guanyl nucleotide binding' and 'guanyl ribonucleotide binding' (Fig. 3D).

Enrichment analysis of KEGG pathway. The results of KEGG pathway enrichment analysis demonstrated that the common DEGs were significantly enriched in the 'Focal adhesion', 'Hippo' and 'Renal cell carcinoma' signaling pathways (Fig. 4).

Analysis of PPI network and hub gene. The PPI network consisted of 167 nodes and 168 edges based on STRING database, and the network was visualized using Cytoscape

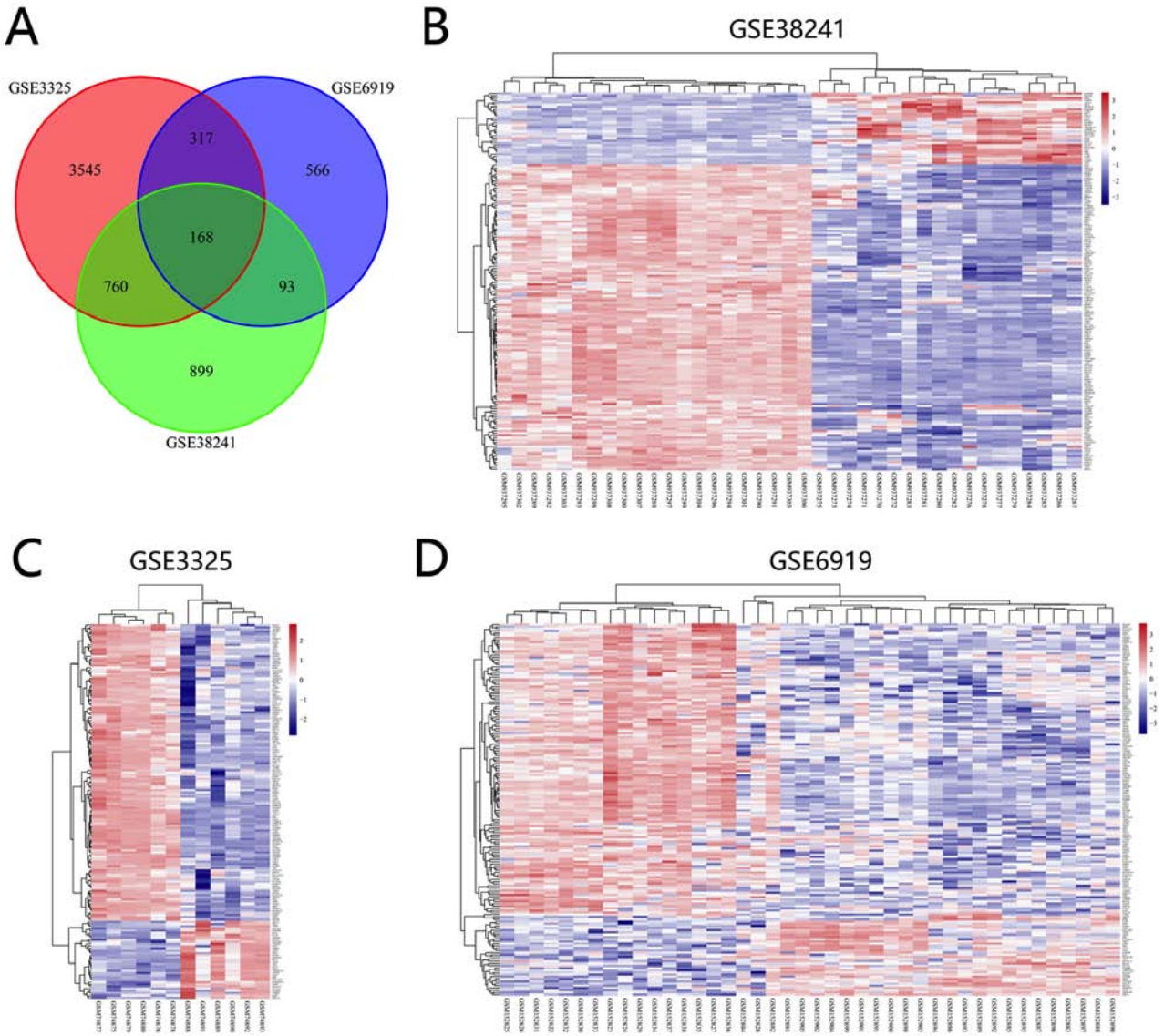

Figure 2. Venn diagram and heatmap of common DEGs. (A) Venn diagram indicates the number of common DEGs in the three datasets. Heatmap of common DEGs in the datasets of (B) GSE38241, (C) GSE3325 and (D) GSE6919. In the heatmap of common DEGs, blue indicates downregulated and red represents upregulated genes. DEG, differentially expressed genes.

software (Fig. 5). The top 10 common DEGs with the highest degree were screened as the hub genes of mPCa and their names and functions are presented in Table I.

Knockdown of PDK1 or PFKFB4 inhibits tumorigenicity of PCa cells in vivo. The BALB/c nude mice were injected subcutaneously with PC-3 cells infected with shRNA-PDK1 or shRNA-PFKFB4. Tumors dissected from mice were imaged and measured (Fig. 6A). The maximum tumor size was 1,775.74 mm^3. It was found that knockdown of PDK1 or PFKFB4 inhibited the tumor growth of PCa cells *in vivo* (Fig. 6B). Similar results were observed for tumor weight (Fig. 6C).

Overexpression of CD44 promotes tumorigenicity of PCa cells in vivo. The BALB/c nude mice were subcutaneously injected with LNCaP cells transfected with CD44 overexpression vector or NC. Tumors dissected from mice were imaged and measured (Fig. 7A). The maximum tumor size was 1,932.95 mm^3. The results indicated that overexpression of CD44 promoted the tumor growth and tumor weight of PCa xenografts *in vivo* (Fig. 7B and C).

Inhibition of CD44 suppresses tumorigenicity of PCa cells in vivo and the CD44 inhibitor (SB-3CT) combined with docetaxel inhibits the tumorigenicity of PCa. The BALB/c nude mice were subcutaneously injected with PC-3 cells. After inoculation, SB-3CT or SB-3CT combined with docetaxel (5 or 10 mg/kg) was injected into mice via the tail vein. Tumors dissected from mice were imaged and measured (Fig. 8A). The maximum tumor size was 1,775.74 mm^3. It was identified that combined therapy with CD44 inhibitor (SB-3CT) and docetaxel could significantly inhibit tumor growth compared with treatment with the CD44 inhibitor (SB-3CT) alone. Moreover, it was found that a high concentration of docetaxel (10 mg/kg) could achieve higher inhibitory effects compared with the low concentration (5 mg/kg) (Fig. 8B and C). The expression levels of PDK1 and PFKFB4 in tumor tissue were examined,

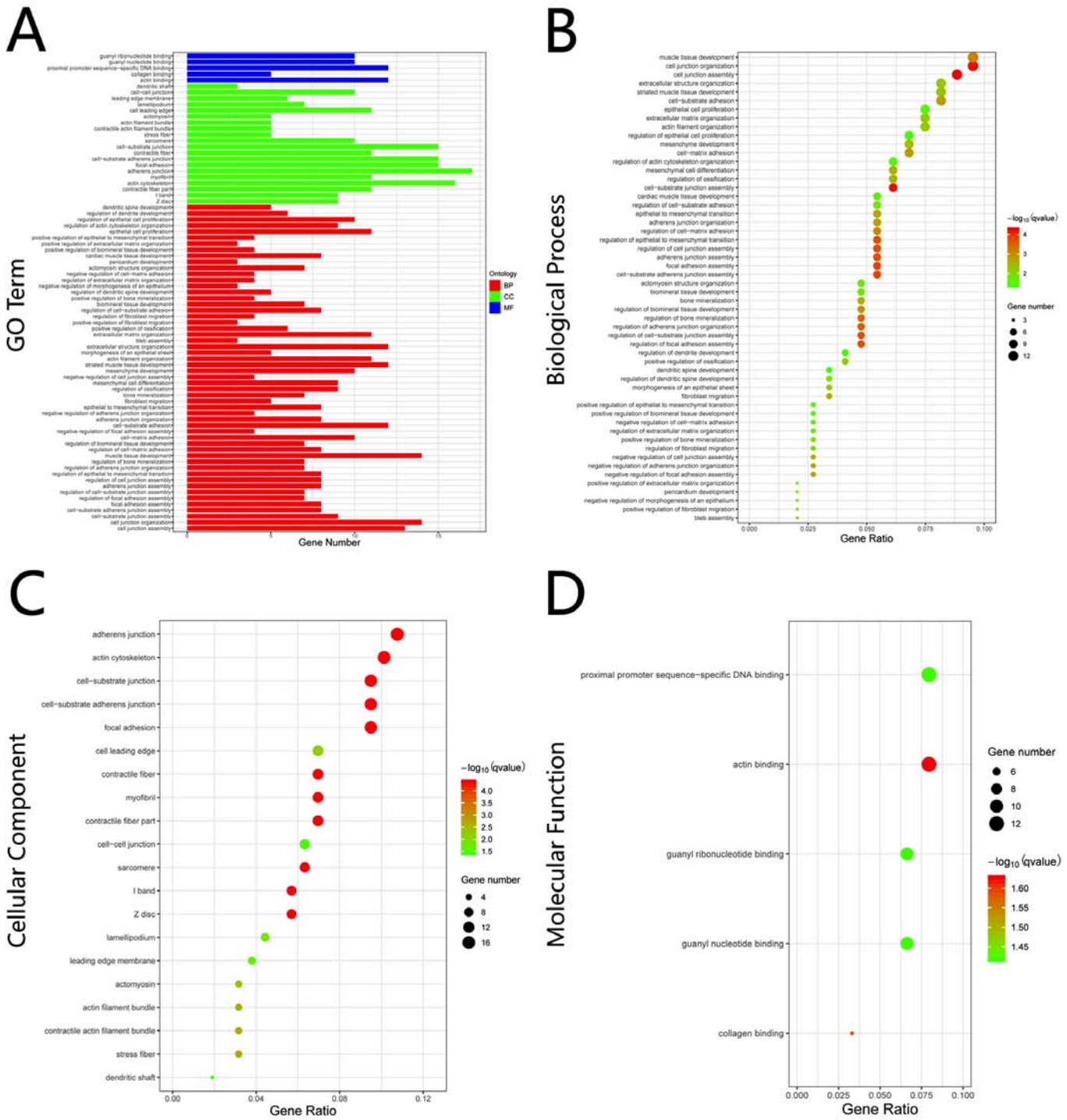

Figure 3. GO enrichment analysis of common DEGs. (A) Results of GO enrichment analysis. The x-axis indicates the number of genes enriched in the marked category. The y-axis represents the functional categories. Only categories of GO with P<0.05 are shown. Bubble charts for (B) BPs, (C) CCs and (D) MFs. The x-axis represents the ratio of common DEGs enriched in the marked category. The size of the bubble indicates the number of common DEGs enriched in the marked category and color refers to the value of difference. GO, Gene Ontology; BP, Biological Processes; CC, Cellular Components; MF, Molecular Functions; DEG, differentially expressed genes.

and were found to be significantly downregulated both in the monotherapy and combined therapy groups. Similar results were also observed in the results of immunohistochemical staining (Fig. 8D-G). Based on these aforementioned results, it was suggested that SB-3CT combined with a high dose of docetaxel could inhibit tumor growth more effectively than SB-3CT alone.

Discussion

Although significant progress has been achieved in the management of mPCa, the pathogenesis of mPCa has not been fully elucidated due to the potentially complex biological traits of cancer. Microarray technology enables researchers to screen hub genes and primary pathways that are associated

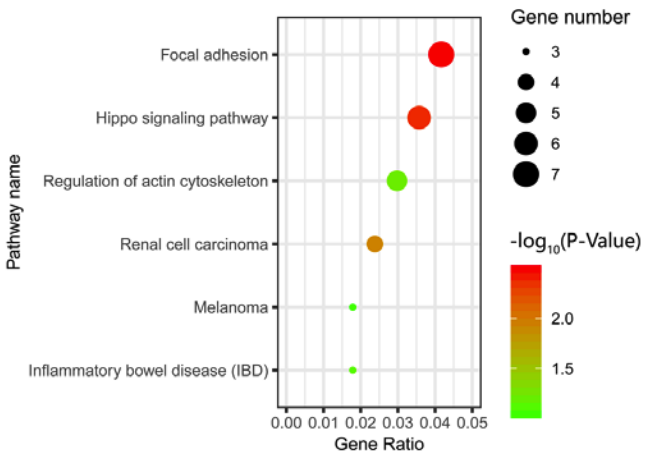

Figure 4. KEGG pathway enrichment analysis of common DEGs. Bubble chart for KEGG pathway enrichment analysis is presented. The x-axis represents the ratio of common DEGs enriched in the marked category. The size of the bubble indicates the number of common DEGs enriched in the marked category and color refers to the value of differences. The categories of 'Focal adhesion', 'Hippo signaling pathway' and 'Renal cell carcinoma' were considered significant, while the categories of 'Regulation of actin cytoskeleton', 'Melanoma' and 'Inflammatory bowel disease' were considered not significant. DEG, differentially expressed genes; KEGG, Kyoto Encyclopedia of Genes and Genomes.

with mPCa, and has proven to be a helpful technology (26). Therefore, microarray technology has been used to identify genetic alterations involved in the pathogenesis and progression of diseases.

In the present study, three microarray databases were accessed to identify DEGs between mPCa tissues and normal prostate tissues. A total of 168 common DEGs were obtained for further analysis. To reveal interactions among the common DEGs, GO and KEGG pathways, enrichment analysis was performed. GO enrichment analysis indicated that the DEGs were mostly enriched in 'cell junction' and 'cell adhesion'. The results of GO analysis are consistent with previous studies, which reported that 'cell junction' is associated with paracellular diffusion regulation and that 'cell adhesion' serves a crucial role in the transformation and progression of cancer (27-29). The KEGG pathway enrichment analysis indicated that the DEGs were mostly enriched in 'Hippo signaling pathway', 'focal adhesion' and 'renal cell carcinoma'. Previous studies have reported that the hippo signaling pathway is involved in the regulation of cell proliferation and cell apoptosis, and is upregulated in tumors (30,31). In the present study, the top 10 common DEGs with highest degree were screened as the hub genes, including PTEN, Rac GTPase-activating protein 1, Protein regulator of cytokinesis 1, PDZ binding kinase, Centromere-associated protein E, NUF2 component of NDC80 kinetochore complex, TPX2 microtubule nucleation factor, SOX2, CD44 and ubiquitin-like with PHD and ring finger domains 1. Previous findings have revealed that CD44 is an adhesion molecule and is involved in the processes of invasion and metastasis in tumor cells (10). The present bioinformatics analysis results were consistent with these aforementioned findings. Based on the current results of the bioinformatics analysis, it was suggested that CD44 could regulate cell proliferation, migration and invasion in PCa.

The results of our previous study revealed that inhibition of CD44 using SB-3CT could suppress proliferation, invasion and migration in PCa cells by regulating PDK1 and PFKFB4 expression levels (12). Based on the present bioinformatics analysis results and our previous study, additional experiments *in vivo* were performed, including tumor formation assay and tumor metastasis experiments. In the present study, the results of tumor xenograft implantation demonstrated that knockdown of PDK1 or PFKFB4 in PC-3 cells inhibited the tumorigenicity of PCa *in vivo*. Further experiments indicated that inhibition of CD44 using an MMP inhibitor (SB-3CT) in PC-3 cells suppressed the tumorigenicity of PCa and inhibited the expression levels of

Table I. Functional roles of top 10 hub genes with a degree ≥8.

No.	Gene symbol	Full name	Function (Ref.)
1	*PTEN*	Phosphatase and tensin homolog	PTEN acts as a tumor suppressor through regulating AKT/PKB signaling pathway negatively (41)
2	*RACGAP1*	Rac GTPase-activating protein 1	RACGAP1 can regulate the progression of cytokinesis, cell growth and differentiation (42)
3	*PRC1*	Protein regulator of cytokinesis 1	PRC1 is associated with cytokinesis (43)
4	*PBK*	PDZ binding kinase	High expression of PBK is associated with tumorigenesis (44)
5	*CENPE*	Centromere-associated protein E	CENPE is necessary for stable spindle microtubule capture (45)
6	*NUF2*	NUF2 component of NDC80 kinetochore complex	NUF2 is associated with centromeres of mitotic (46)
7	*TPX2*	TPX2 microtubule nucleation factor	TPX2 is implicated as a regulator of cell apoptosis (47)
8	*SOX2*	SRY-box transcription factor 2	Transcription factors encoded by SOX2 play a regulatory role in embryonic development (48)
9	*CD44*	CD44 molecule	CD44 is associated with cell-cell interaction, cell migration and adhesion (10)
10	*UHRF1*	Ubiquitin-like with PHD and ring finger domains 1	UHRF1 is overexpressed in various types of cancer (49)

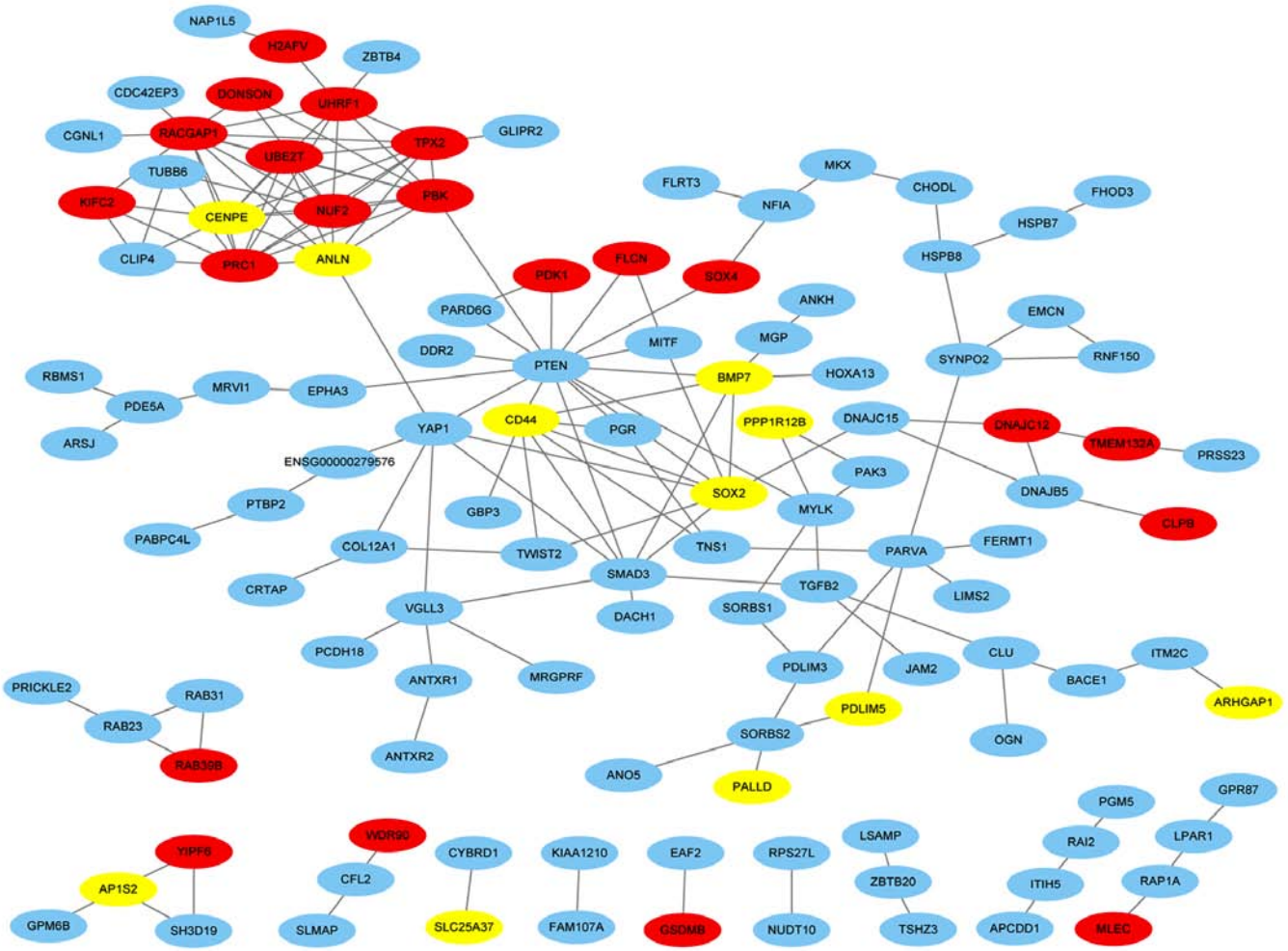

Figure 5. PPI network and module analysis of common DEGs. A total of 167 DEGs were screened using the STRING database and the PPI network was constructed using Cytoscape. The color is indicative of the different genes: Blue represents downregulated genes, while red indicates upregulated genes. Yellow represents genes that are upregulated in some probes but downregulated in other probes. DEG, differentially expressed genes; PPI, protein-protein interaction.

PDK1 and PFKFB4 in PC-3 cells. SB-3CT, a selective MMP inhibitor, has been reported to block CD44 cleavage and inhibit downstream signaling pathway (32). Taken together, the present results indicated that CD44 suppressed the tumorigenicity of PCa via PDK1 and PFKFB4 *in vivo*, which was consistent with the results of previous study *in vitro* (12). As aforementioned, previous studies have reported that PC-3 cells expressed CD44, while LNCaP cells did not (11). In the present study, CD44 was overexpressed in LNCaP cells and this overexpression promoted the tumorigenicity of PCa. Tumor metastasis experiments were also performed. In the present study, metastatic tumors were found in the lung of the mice. However, the difference between two groups in the number of metastatic tumors in the lung was not significant.

Currently, hormonal therapy and chemotherapy are the first line choice for the treatment of mPCa, and adverse events were frequent in the two protocols (33). The combination of hormonal therapy and docetaxel became a novel therapy for mPCa. The results of the present study demonstrated that CD44 regulated the tumorigenicity of PCa *in vivo*, which suggested that inhibition of CD44 using SB-3CT is a novel potential treatment of PCa. According to current combined therapy of mPCa, it was suggested that the combination of CD44 inhibitor and docetaxel may be a beneficial strategy. Our previous study revealed that the combination of docetaxel and SB-3CT could significantly decrease the viability of PC-3 cells compared with single treatment of docetaxel at the concentration of 5 or 10 mg/kg (12). The present study evaluated the effect of combined therapy with CD44 inhibitor (SB-3CT) and docetaxel. The results indicated that treatment with CD44 inhibitor and docetaxel inhibited tumor growth and decreased expression levels of PDK1 and PFKFB4. Moreover, it was identified that treatment with high concentration of docetaxel induced a more positive response compared with the low concentration. Although the combined therapy was effective, sequential therapy is another potential therapy, but requires further investigation (34).

CD44 is a cell-surface receptor for hyaluronic acid and extracellular matrix components, and it serves a critical role in connecting the microenvironments in cancer. CD44 enables cancer cells to perceive the changes of microenvironments and can mediate the transduction of growth factor and cytokine signaling which can promote cell invasion and metastasis. Growth factors from microenvironments mediated by CD44,

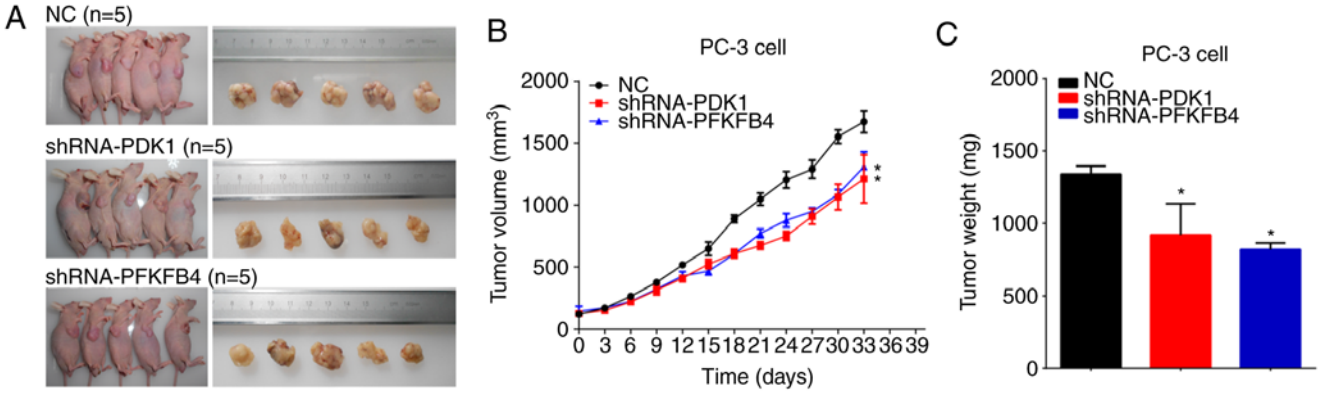

Figure 6. Knockdown of PDK1 or PFKFB4 inhibits tumorigenicity of prostate cancer cells *in vivo*. (A) Tumors dissected from 15 BALB/c nude mice are presented (n=5 for each group). (B) Tumor volume curve of NC, PDK1 and PFKFB4 treatment groups. Asterisk in the red tumor volume curve indicates that the shRNA-PDK1 group is significantly different compared to the NC group. Asterisk in the blue tumor volume curve indicates that the shRNA-PFKFB4 group is significantly different compared to the NC group. (C) Tumor weight of NC, PDK1 and PFKFB4 treatment groups. Knockdown of PDK1 or PFKFB4 inhibited the tumor growth of prostate cancer cells *in vivo*. Data are analysed using an ANOVA with Tukey's post hoc test. Data are presented as the mean ± SD. *P<0.05. NC, negative control; PDK1, pyruvate dehydrogenase kinase 1; PFKB4, 6-phosphofructo-2-kinase/fructose-2,6-biphosphatase 4.

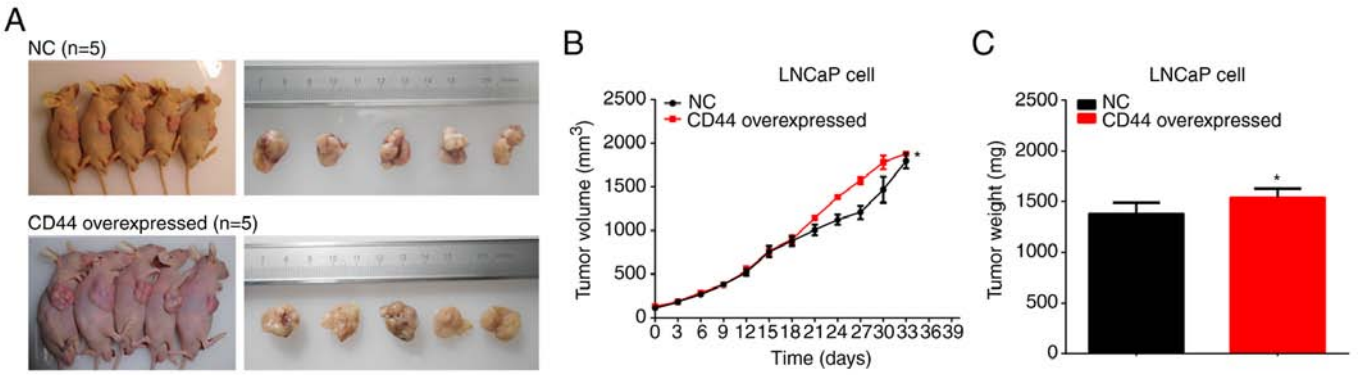

Figure 7. Overexpression of CD44 promotes tumorigenicity of prostate cancer cells *in vivo*. (A) Tumors dissected from 10 BALB/c nude mice are presented (n=5 for each group). (B) Tumor volume curve of NC and CD44 treatment groups. (C) Tumor weight of NC and CD44 treatment groups. Overexpression of CD44 promoted the tumor growth of prostate cancer cells *in vivo*. Data are analysed using a Student's t-test (independent t-test) or an ANOVA with Tukey's post hoc test. Data are presented as the mean ± SD. *P<0.05. NC, negative control; PDK1, pyruvate dehydrogenase kinase 1; PFKB4, 6-phosphofructo-2-kinase/fructose-2,6-biphosphatase 4.

including EDF, FGF, HGF, VEGF, TGF-β, can also regulate tumorigenicity (35). It has been reported that CD44 could regulate the activation of macrophages in tumors, which was associated with tumorigenicity (36,37). As aforementioned, the regulation of microenvironments or macrophages by CD44 could affect tumorigenicity, but this required further examination. CD44 can also regulate EMT and reactive oxygen species (ROS) metabolism. Moreover, CD44 may regulate glucose metabolism in PCa (38). With increased glycolytic activity, reduced mitochondrial respiration leads to decreased ROS levels (39). Previous *in vitro* studies have reported that inhibition of CD44 expression could decrease glucose consumption and increase ROS level. Based on these results, it was suggested that CD44 could regulate the tumorigenicity of PCa cells via the regulation of ROS via PDK1 or PFKFB4.

The 70-kDa ribosomal protein S6 kinase, known as p70S6K, is a dual pathway kinase which acts downstream of PI3K pathway and mTOR pathway in response to growth factors and cytokines to regulate cell growth and inhibit cell apoptosis. Previous findings showed that p70S6K was regulated by PDK1 in PI3K pathway and could suppress BAD-induced cell apoptosis by the phosphorylation of Ser-136 on BAD (40). In our study, it was suggested that CD44 could suppress the tumorigenicity of prostate cancer by decreasing PDK1 and PFKFB4. Consequently, we hypothesized that CD44 could regulate the apoptosis of prostate cancer cells through p70S6K. In future, the effect of CD44 on the apoptosis of prostate cancer and its mechanism may be the focus of future research.

However, the present study has some limitations. CD44 has two variable regions and various CD44 isoforms produced by alternative splicing, which may have diverse effects on cancer progression. Thus, the CD44 isoforms should be analyzed and examined further in PCa tissues. Our previous findings demonstrated the difference between combined treatment and docetaxel alone *in vitro*. In addition, docetaxel was the first-line treatment for castration-resistant prostate cancer, which had been confirmed by lots of experiments *in vivo* and clinical practices. The main purpose of the present study was confirming the benefits of combined treatment with docetaxel and SB-3CT, a novel compound for prostate cancer treatment. Based on the

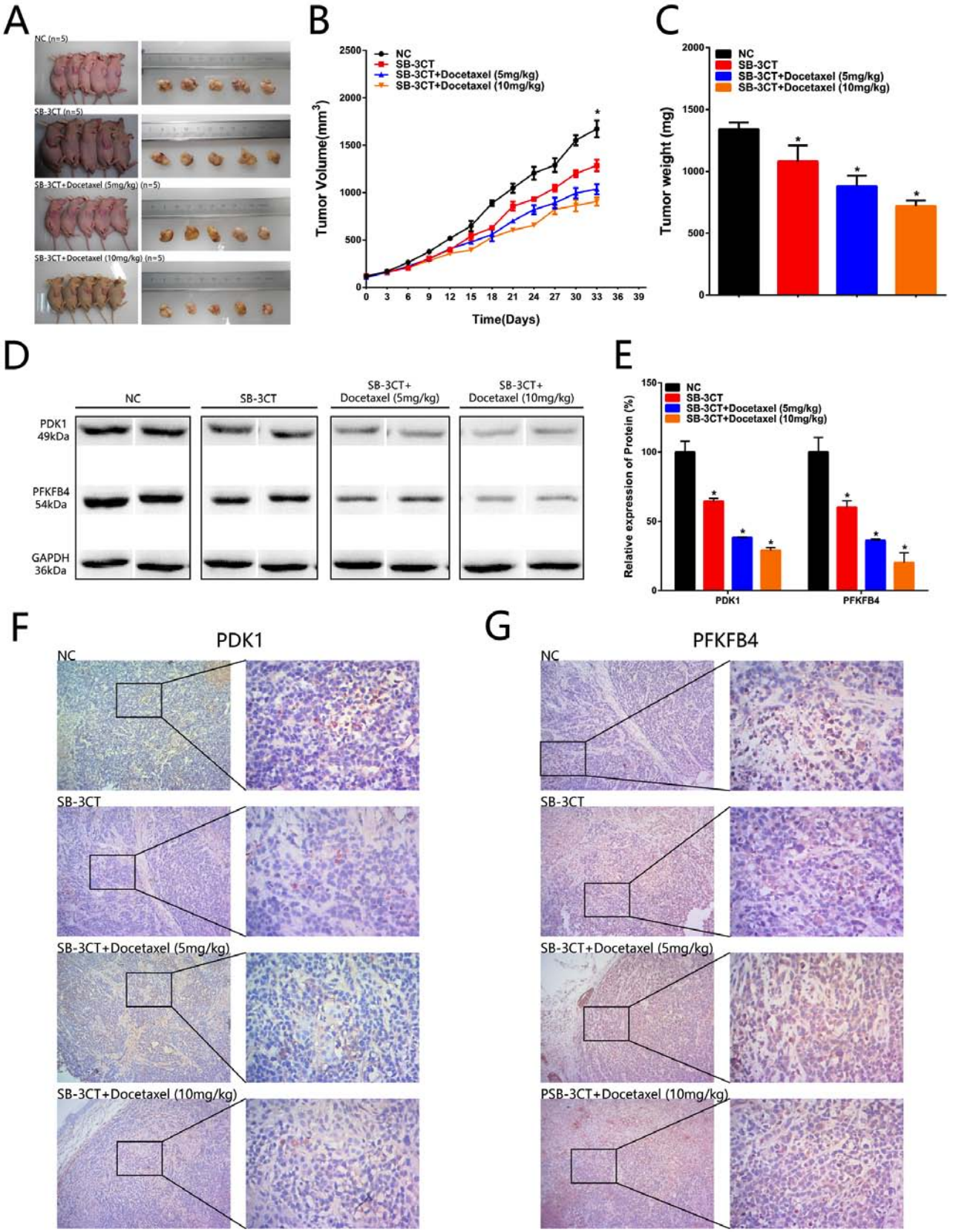

Figure 8. Inhibition of CD44 suppresses tumorigenicity of prostate cancer cells *in vivo* and the CD44 inhibitor (SB-3CT) combined with docetaxel inhibits tumorigenicity of prostate cancer. (A) Tumors dissected from BALB/c nude mice are presented (n=5 for each group). (B) Tumor volume curve of NC, SB-3CT, SB-3CT + Docetaxel (5 mg/kg) and SB-3CT + Docetaxel (10 mg/kg) treatment groups. (C) Tumor weight of NC, SB-3CT, SB-3CT + Docetaxel (5 mg/kg) and SB-3CT + Docetaxel (10 mg/kg) treatment groups. (D and E) PDK1 and PFKFB4 expression levels were downregulated in the PC-3 + SB-3T group, PC-3 + SB-3T + Docetaxel (5 mg/kg) group and PC-3 + SB-3T + Docetaxel (10 mg/kg) group compared with the PC-3 + NC group. (F) PDK1 expression levels were downregulated in the PC-3 + SB-3T group, PC-3 + SB-3T + Docetaxel (5 mg/kg) group and PC-3 + SB-3T + Docetaxel (10 mg/kg) group compared with the PC-3 + NC group. (G) PFKFB4 expression levels were downregulated in the PC-3 + SB-3T group, PC-3 + SB-3T + Docetaxel (5 mg/kg) group and PC-3 + SB-3T + Docetaxel (10 mg/kg) group compared with the PC-3 + NC group. Data are analysed using an ANOVA with Tukey's post hoc test. Data are presented as the mean ± SD. *P<0.05. NC, negative control; PDK1, pyruvate dehydrogenase kinase 1; PFKB4, 6-phosphofructo-2-kinase/fructose-2,6-biphosphatase 4.

aforementioned findings, SB-3CT alone was designed as the control group; however, it would be more reasonable to add docetaxel as monotherapy as a further control group.

In conclusion, a total of 168 common DEGs were identified and 10 hub genes were considered as biomarkers for mPCa. Further experimental results indicated that CD44 regulated the tumorigenicity of PCa via PDK1 and PFKFB4 *in vivo*. The present results demonstrated that the combination of SB-3CT and docetaxel was more effective in the inhibition of tumor growth, which suggested that combination therapy is a potential therapeutic strategy for mPCa.

Acknowledgements

Not applicable.

Funding

This work was funded by the National Natural Science Foundation of China (grant no. 81460387).

Availability of data and materials

The data are available on reasonable request from the corresponding author.

Authors' contributions

WL contributed to the experiment conception and design, data analysis, and manuscript draft. JL, ZC, and XL conducted the experiments. WL, JL, DN, and GH contributed to manuscript draft and data analysis. NH, ZL, and JL contributed to interpretation of data, manuscript draft and manuscript revision. NH, ZL, and JL are responsible for confirming the authenticity of all the raw data. All authors read and approved the final manuscript.

Ethics approval and consent to participate

The Ethics Committee of the People's Hospital of Guangxi Zhuang Autonomous Region approved the study (approval no. 2014-010). Informed consent was provided by all the participants.

Patient consent for publication

Not applicable.

Competing interests

The authors declare that they have no competing interests.

References

1. Bray F, Ferlay J, Soerjomataram I, Siegel RL, Torre LA and Jemal A: Global cancer statistics 2018: GLOBOCAN estimates of incidence and mortality worldwide for 36 cancers in 185 countries. CA Cancer J Clin 68: 394-424, 2018.
2. Cocci A, Cito G, Romano A, Larganà G, Vignolini G, Minervini A, Di Maida F, Campi R, Carini M, Mondaini N and Russo GI: Radical prostatectomy and simultaneous penile prosthesis implantation: A narrative review. Int J Impot Res 32: 274-280, 2020.
3. Weiner AB, Nettey OS and Morgans AK: Management of metastatic hormone-sensitive prostate cancer (mHSPC): An evolving treatment paradigm. Curr Treat Options Oncol 20: 6, 2019.
4. Heidenreich A, Bastian PJ, Bellmunt J, Bolla M, Joniau S, van der Kwast T, Mason M, Matveev V, *et al*: EAU guidelines on prostate cancer. Part II: Treatment of advanced, relapsing, and castration-resistant prostate cancer. Eur Urol 65: 467-479, 2014.
5. Wülfing C, Bögemann M, Goebell PJ, Hammerer P, Machtens S, Pfister D, Schwentner C, Steuber T, von Amsberg G and Schostak M: Treatment situation in metastastic Castration Naive Prostate Cancer (mCRPC) and the implications on clinical routine. Urologe A 58: 1066-1072, 2019 (In German).
6. Dailey AL:Metabolomic bioinformatic analysis. Methods Mol Biol 1606: 341-352, 2017.
7. Spring FA, Dalchau R, Daniels GL, Mallinson G, Judson PA, Parsons SF, Fabre JW and Anstee DJ: The Ina and Inb blood group antigens are located on a glycoprotein of 80,000 MW (the CDw44 glycoprotein) whose expression is influenced by the In(Lu) gene. Immunology 64: 37-43, 1988.
8. Prochazka L, Tesarik R and Turanek J: Regulation of alternative splicing of CD44 in cancer. Cell Signal 26: 2234-2239, 2014.
9. Miletti-González KE, Murphy K, Kumaran MN, Ravindranath AK, Wernyj RP, Kaur S, Miles GD, Lim E, Chan R, Chekmareva M, *et al*: Identification of function for CD44 intracytoplasmic domain (CD44-ICD). J Biol Chem 287: 18995-19007, 2012.
10. Nagano O and Saya H: Mechanism and biological significance of CD44 cleavage. Cancer Sci 95: 930-935, 2004.
11. Tai S, Sun Y, Squires JM, Zhang H, Oh WK, Liang CZ and Huang J: PC3 is a cell line characteristic of prostatic small cell carcinoma. Prostate 71: 1668-1679, 2011.
12. Li W, Qian L, Lin J, Huang G, Hao N, Wei X, Wang W and Liang J: CD44 regulates prostate cancer proliferation, invasion and migration via PDK1 and PFKFB4. Oncotarget 8: 65143-65151, 2017.
13. Barrett T, Wilhite SE, Ledoux P, Evangelista C, Kim IF, Tomashevsky M, Marshall KA, Phillippy KH, Sherman PM, Holko M, *et al*: NCBI GEO: Archive for functional genomics data sets-update. Nucleic Acids Res 41 (Database Issue): D991-D995, 2013.
14. Edgar R, Domrachev M and Lash AE: Gene Expression Omnibus: NCBI gene expression and hybridization array data repository. Nucleic Acids Res 30: 207-210, 2002.
15. Varambally S, Yu J, Laxman B, Rhodes DR, Mehra R, Tomlins SA, Shah RB, Chandran U, Monzon FA, Becich MJ, *et al*: Integrative genomic and proteomic analysis of prostate cancer reveals signatures of metastatic progression. Cancer Cell 8: 393-406, 2005.
16. Chandran UR, Ma C, Dhir R, Bisceglia M, Lyons-Weiler M, Liang W, Michalopoulos G, Becich M and Monzon FA: Gene expression profiles of prostate cancer reveal involvement of multiple molecular pathways in the metastatic process. BMC Cancer 7: 64, 2007.
17. Yu YP, Landsittel D, Jing L, Nelson J, Ren B, Liu L, McDonald C, Thomas R, Dhir R and Finkelstein S: Gene expression alterations in prostate cancer predicting tumor aggression and preceding development of malignancy. J Clin Oncol 22: 2790-2799, 2004.
18. Aryee MJ, Liu W, Engelmann JC, Nuhn P, Gurel M, Haffner MC, Esopi D, Irizarry RA, Getzenberg RH, Nelson WG, *et al*: DNA methylation alterations exhibit intraindividual stability and interindividual heterogeneity in prostate cancer metastases. Sci Transl Med 5: 169ra10, 2013.
19. Smyth GK: Linear models and empirical bayes methods for assessing differential expression in microarray experiments. Stat Appl Genet Mol Biol 3: Article3, 2004.
20. Yu G, Wang LG, Han Y and He QY: clusterProfiler: An R package for comparing biological themes among gene clusters. OMICS 16: 284-287, 2012.
21. Huang da W, Sherman BT and Lempicki RA: Systematic and integrative analysis of large gene lists using DAVID bioinformatics resources. Nat Protoc 4: 44-57, 2009.
22. Huang da W,Sherman BT and Lempicki RA: Bioinformatics enrichment tools: Paths toward the comprehensive functional analysis of large gene lists. Nucleic Acids Res 37: 1-13, 2009.
23. Shannon P, Markiel A, Ozier O, Baliga NS, Wang JT, Ramage D, Amin N, Schwikowski B and Ideker T: Cytoscape: A software environment for integrated models of biomolecular interaction networks. Genome Res 13: 2498-2504, 2003.
24. Szklarczyk D,Gable AL,Lyon D,Junge A,Wyder S,Huerta-Cepas J, Simonovic M, Doncheva NT, Morris JH, Bork P, *et al*: STRING v11: Protein-protein association networks with increased coverage, supporting functional discovery in genome-wide experimental datasets. Nucleic Acids Res 47: D607-D613, 2019.

25. Chin CH, Chen SH, Wu HH, Ho CW, Ko MT and Lin CY: cytoHubba: Identifying hub objects and sub-networks from complex interactome. BMC Syst Biol 8 (Suppl 4): S11, 2014.
26. Albertson DG and Pinkel D: Genomic microarrays in human genetic disease and cancer. Hum Mol Genet 12 Spec No 2: R145-R152, 2003.
27. Hejmej A and Bilinska B: A role of junction-mediated interactions in cells of the male reproductive tract: Impact of prenatal, neonatal, and prepubertal exposure to anti-androgens on adult reproduction. Histol Histopathol 29: 815-830, 2014.
28. Hejmej A and Bilinska B: The effects of flutamide on cell-cell junctions in the testis, epididymis, and prostate. Reprod Toxicol 81: 1-16, 2018.
29. Yu CC, Chen LC, Lin VC, Huang CY, Cheng WC, Hsieh AR, Chang TY, Lu TL, Lee CH, Huang SP and Bao BY: Effect of genetic variants in cell adhesion pathways on the biochemical recurrence in prostate cancer patients with radical prostatectomy. Cancer Med 8: 2777-2783, 2019.
30. Pan D: The hippo signaling pathway in development and cancer. Dev Cell 19: 491-505, 2010.
31. Saucedo LJ and Edgar BA: Filling out the Hippo pathway. Nat Rev Mol Cell Biol 8: 613-621, 2007.
32. Thorne RF, Legg JW and Isacke CM: The role of the CD44 transmembrane and cytoplasmic domains in co-ordinating adhesive and signalling events. J Cell Sci 117: 373-380, 2004.
33. Tannock IF, de Wit R, Berry WR, Horti J, Pluzanska A, Chi KN, Oudard S, Théodore C, James ND, Turesson I, *et al*: Docetaxel plus prednisone or mitoxantrone plus prednisone for advanced prostate cancer. N Engl J Med 351: 1502-1512, 2004.
34. Takeuchi H, Mmeje CO, Jinesh GG, Taoka R and Kamat AM: Sequential gemcitabine and tamoxifen treatment enhances apoptosis and blocks transformation in bladder cancer cells. Oncol Rep 34: 2738-2744, 2015.
35. Yan Y, Zuo X and Wei D: Concise review: Emerging role of CD44 in cancer stem cells: A promising biomarker and therapeutic target. Stem Cells Transl Med 4: 1033-1043, 2015.
36. Rao G, Wang H, Li B, Huang L, Xue D, Wang X, Jin H, Wang J, Zhu Y, Lu Y, *et al*: Reciprocal interactions between tumor-associated macrophages and CD44-positive cancer cells via Osteopontin/CD44 promote tumorigenicity in colorectal cancer. Clin Cancer Res 19: 785-797, 2012.
37. Takeuchi H, Tanaka M, Tanaka A, Tsunemi A and Yamamoto H: Predominance of M2-polarized macrophages in bladder cancer affects angiogenesis, tumor grade and invasiveness. Oncol Lett 11: 3403-3408, 2016.
38. Li W, Cohen A, Sun Y, Squires J, Braas D, Graeber TG, Du L, Li G, Li Z, Xu X, *et al*: The role of CD44 in glucose metabolism in prostatic small cell neuroendocrine carcinoma. Mol Cancer Res 14: 344-353, 2016.
39. Takeuchi H, Taoka R, Mmeje CO, Jinesh GG, Safe S and Kamat AM: CDODA-Me decreases specificity protein transcription factors and induces apoptosis in bladder cancer cells through induction of reactive oxygen species. Urol Oncol 34: 337.e11-e18, 2016.
40. Harada H, Andersen JS, Mann M, Terada N and Korsmeyer SJ: p70S6 kinase signals cell survival as well as growth, inactivating the pro-apoptotic molecule BAD. Proc Natl Acad Sci USA 98: 9666-9670, 2001.
41. Chu EC and Tarnawski AS: PTEN regulatory functions in tumor suppression and cell biology. Med Sci Monit 10: RA235-RA241, 2004.
42. Glotzer M: Cytokinesis: Centralspindlin moonlights as a membrane anchor. Curr Biol 23: R145-R147, 2013.
43. Jiang W, Jimenez G, Wells NJ, Hope TJ, Wahl GM, Hunter T and Fukunaga R: PRC1: A human mitotic spindle-associated CDK substrate protein required for cytokinesis. Mol Cell 2: 877-885, 1998.
44. Gaudet S, Branton D and Lue RA: Characterization of PDZ-binding kinase, a mitotic kinase. Proc Natl Acad Sci USA 97: 5167-5172, 2000.
45. Testa JR, Zhou JY, Bell DW and Yen TJ: Chromosomal localization of the genes encoding the kinetochore proteins CENPE and CENPF to human chromosomes 4q24->q25 and 1q32->q41, respectively, by fluorescence in situ hybridization. Genomics 23: 691-693, 1994.
46. Nabetani A, Koujin T, Tsutsumi C, Haraguchi T and Hiraoka Y: A conserved protein, Nuf2, is implicated in connecting the centromere to the spindle during chromosome segregation: A link between the kinetochore function and the spindle checkpoint. Chromosoma 110: 322-334, 2001.
47. Holland AJ and Cleveland DW: Losing balance: The origin and impact of aneuploidy in cancer. EMBO Rep 13: 501-514, 2012.
48. Johansson H and Simonsson S: Core transcription factors, Oct4, Sox2 and Nanog, individually form complexes with nucleophosmin (Npm1) to control embryonic stem (ES) cell fate determination. Aging (Albany NY) 2: 815-822, 2010.
49. Mudbhary R, Hoshida Y, Chernyavskaya Y, Jacob V, Villanueva A, Fiel MI, Chen X, Kojima K, Thung S, Bronson RT, *et al*: UHRF1 overexpression drives DNA hypomethylation and hepatocellular carcinoma. Cancer Cell 25: 196-209, 2014.